50TH EASTERN SNOW CONFERENCE
61ST WESTERN SNOW CONFERENCE
Quebec City 1993

Snowdrift Modeling in the CRREL Wind Tunnel

R.B. HAEHNEL, CPT. J.H. WILKINSON AND J.H. LEVER
Ice Engineering Research Branch
U.S. Army Cold Regions Research and Engineering Laboratory
72 Lyme Road
Hanover, New Hampshire 03755-1290 U.S.A.

ABSTRACT

We modified CRREL's Snow Drifting Wind Tunnel to generate a flow field that simulates the atmospheric boundary layer and installed a trap for measuring the average mass flux. We replaced the previously used activated clay with glass beads and developed a moiré photography system to measure drift profile.

We then conducted a series of preliminary calibration tests to verify the similarity of model and full-scale snowdrifts. Two-dimensional calibrations included a Wyoming snow fence and a step. Three-dimensional tests included a right circular cylinder and a rectangular prism. Generally, the agreement was good between model and prototype drift geometries. However, there is insufficient quantitative field data availible to thouroughly validate the model results.

INTRODUCTION

Drifting snow presents problems for transportation and building technologies. It reduces visibility and can deposit on roadways and railways, making transportation dangerous or impossible. Snow drifting around buildings can cause roofs to fail, block air intakes, and render access-ways inoperable. The aim of snowdrift simulation is to predict depth, location, and rate of accumulation of drifts around structures.

In 1985, CRREL built a Snow Drifting Wind Tunnel (SDWT) for physical modeling of drifting problems. This tunnel was a closed loop recirculating wind tunnel with a cross section of 0.51 m x 0.51 m. Activated clay was used as the modeling medium (see Anno (1987)). The SDWT was modified in 1987 by making the test section longer and installing glass doors on the test section (see Figure 1). Described here are additional improvements made to the SDWT, including a change in model snow material, and results of preliminary model validation tests.

SNOWDRIFT MODELING CRITERIA

Mellor (1965), Kind (1981), and Tabler et al. (1990) provide detailed descriptions of snow drifting processes. We present a summary here. Essentially, drifting snow is the result of wind interaction with the loosely bonded snow particles. Movement occurs when the wind shear stress, τ, exceeds the gravitational and cohesive forces acting to restrain the particles. The corresponding threshold wind speed is dependent on snow cohesion, particle size, and the aerodynamic roughness of the surface, Z_0 (see Schmidt [1980]).

Wind speeds at or just above the threshold provide just enough energy to roll one particle over another. This is termed creep. As the wind speed increases, particles are ejected from the snow surface and carried some distance downwind before they splash back into the bed and knock other particles loose. This is known as saltation. Photographs taken by Kobayashi (1972) show the saltation layer to be 1 to 2 cm thick. Some of the saltating particles will interact with the turbulent flow above the saltation layer. If the turbulent eddies have vertical velocities in excess of the particle terminal velocity, u_f, particles can be swept up several meters into the air by turbulent diffusion.

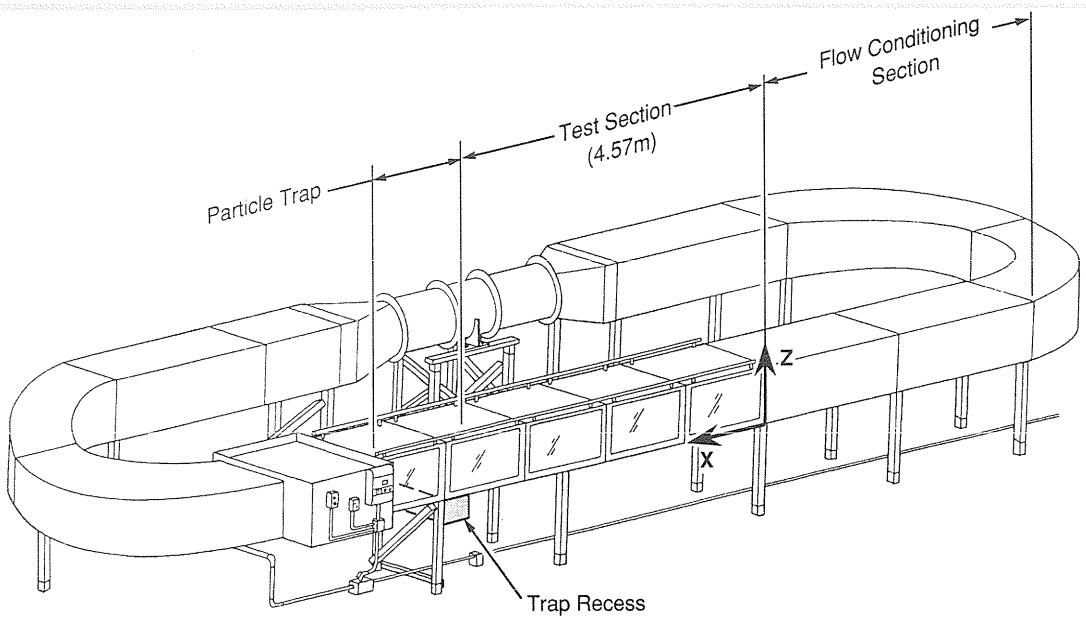

Figure 1. The CRREL Snow Drifting Wind Tunnel.

Typically creep, saltation, and turbulent diffusion occur simultaneously in the flow, with creep only contributing slightly to the total transport. The proportion of snow being transported by each of these mechanisms is determined by wind speed, snow hardness, and particle size.

The wind incident to the snow fetch is part of the planetary boundary layer. The mean velocity, U_Z, is one dimensional in the cross-wind direction and increases with elevation, Z, according to

$$U_Z = \frac{u_*}{K} \ln\left(\frac{Z}{Z_0}\right) \qquad (1)$$

where u_* is the shear velocity ($u_* \equiv \sqrt{\tau/\rho}$), ρ is the air density, and K is von Kármán's constant (~0.4). Teunissen (1970) shows that the longitudinal turbulence varies with elevation according to

$$\frac{u'}{U_Z} = \frac{C}{\ln\frac{Z}{Z_o}} \qquad (2)$$

where u' is the rms velocity and C is about unity for the longitudinal turbulence intensity.

To predict the correct time-dependent development of snowdrifts around structures, model drifts must (a) be geometrically similar to those at full scale and (b) develop at a rate that scales in a known manner. Many authors, including Wuebben (1978), Iversen (1979), Tabler (1980b), Anno (1984), and Kind (1986) have reviewed similitude requirements for snow drifting. We summarize these requirements below.

Condition (a), geometric similitude of snowdrifts, requires kinematic similitude of model and prototype wind fields because wind shear stress governs erosion and deposition of snow particles. Wind-field similitude is achieved through standard wind engineering requirements (see Simiu and Scanlan [1978]) namely:

1. Geometric scaling of model and nearby terrain,
2. Correct velocity profile in the approaching wind, and
3. Fully rough flow around the structures of interest.

The first requirement is simple to meet by correct model construction. The second requirement demands a fully developed/fully turbulent boundary layer with a velocity profile characterized by equation 1. Kind (1976) suggests that

$$\frac{u_*^3}{2g\nu} \gtrsim 30 \qquad (3)$$

assures fully turbulent flow, and

$$\left[\frac{Z_o'}{L}\right]_m = \left[\frac{Z_o'}{L}\right]_p \qquad (4)$$

is the similitude parameter for equation 1. Here, ν is kinematic viscosity, g is the gravitational constant, Z'_o is the aerodynamic roughness of saltation, L is some characteristic length, and m and p denote model and prototype, respectively.

For sharp-edged bluff bodies, the flow around them is largely Reynolds number independent, and requirement 3 is easily met. For rounded bodies, however, the flow is highly Reynolds number

dependent and the flow around the model is too smooth in comparison to prototype. Hence, rounded models are often fitted with sand paper or small wires to roughen the flow (see Simiu and Scanlan (1978)).

Meeting condition (b), time scaling of drift development, is more demanding and requires similitude of the forces predominating snow transport:

4. The ratio of wind shear stress to particle resistance to motion
5. The ratio of uplift force to gravitational force and,
6. The ratio of inertial force to gravitational force.

Requirement 4 is met if the ratio of friction speed to threshold friction speed (u_*/u_{*_t}) is maintained between model and prototype. Requirement 5 is satisfied if the ratio of friction speed to fall velocity (u_*/u_f) is preserved. When requirements 4 and 5 are met simultaneously (u_f/u_{*_t}) the proportion of snow transported by saltation and diffusion as a function of wind speed is preserved between model and prototype. Requirement 6 assures particle trajectories scale with structure dimensions, and can be satisfied by preserving

$$F = \frac{U^2}{Lg}\frac{\sigma}{\sigma-\rho} \qquad (5)$$

where F is the densimetric Froude number, σ is the particle density, and L is a characteristic length.

Other similitude requirements are generally less important than these six. Distortion of particle size, for example, should not adversely affect drift similitude, provided the particle diameter is very small in comparison to the saltation-layer thickness. Additionally, angle of repose similitude can be relaxed when steep slopes are not the main area of concern.

If we satisfy requirements 1-6, model snow drifting should be dynamically similar to full-scale snow drifting. Hence, particle capture efficiencies should be the same in model and prototype for similar geometries. In such a case, the rate of drift development would be proportional to the drift mass divided by the incident mass flux or

$$\left[\frac{L^2\rho_b}{tq}\right]_m = \left[\frac{L^2\rho_b}{tq}\right]_p \qquad (6)$$

where t is the time to develop a drift, q is the incident mass flux ($gm^{-1}s^{-1}$) and ρ_b is the bulk particle density. Similar expressions for scaling time have been developed by Kind (1976) and Anno (1984).

For heavy particles (e.g., glass beads) in air, five of the six principal scaling requirements can be met quite closely. However, Froude number similitude is difficult to achieve in air flow. This is because most model studies examine snow drifting around relatively large sites, demanding use of small geometric scales. In air flow, velocities would need to drop as the square root of the length scale to maintain Froude number similitude. Yet, minimum Reynolds number requirements and minimum threshold speeds prevent large reductions in flow velocities. Thus, relative particle trajectories in wind tunnels are generally larger than prototype values, and as a result model particles may overshoot a wake region behind a structure that prototype particles fall into. This reduces the rate of model drift development in comparison with full-scale rates. While Anno (1984), Kind (1986), and others suggest that Froude number distortion is tolerable provided trajectories remain small relative to structural dimensions, this may be difficult to ensure for models smaller than about 1:50.

All scaling formulations, including this one, characterize the complex snow drifting process using a few key requirements. *Even without distortion in any parameters, these formulations must be verified against full-scale data.* With some parameters distorted, such as Froude number, the need for full-scale verification is even greater. This will require field data with simultaneous drift geometry and mass flux measurements. Unfortunately, such field data are not available.

Comparing model and prototype equilibrium drift geometries represents a less demanding verification approach. Unfortunately, measurements of full-scale equilibrium drift geometries are also rare, with snow fences being best documented (Tabler [1980a]). Consequently, we added to the available field data by conducting some field measurements to verify our model formulation.

WIND TUNNEL MODIFICATIONS

Flow Field Simulation

We improved the velocity profile entering the test section by installing several metal screens. We then found that a velocity profile consistent with equation 1 developed naturally over the simulated snow in about 3 m. Figure 2 shows that the velocity follows a log linear profile up to 10 cm, an adequate height for our small wind tunnel. This velocity similitude is maintained over the SDWT's operational range of 0 to 10 m/s. We also found the turbulence intensity in the wind tunnel follows

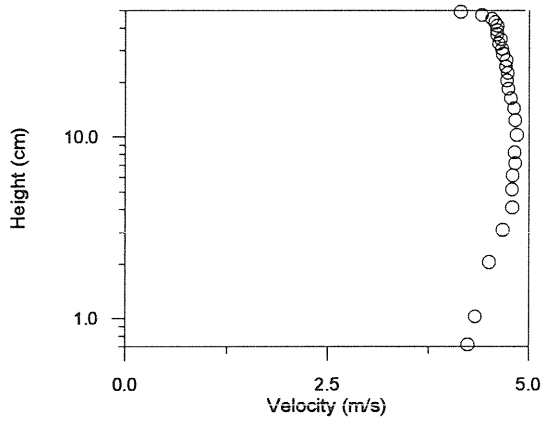

Figure 2. Vertical velocity profile in the CRREL Snow Drifting Wind Tunnel with drifting snow.

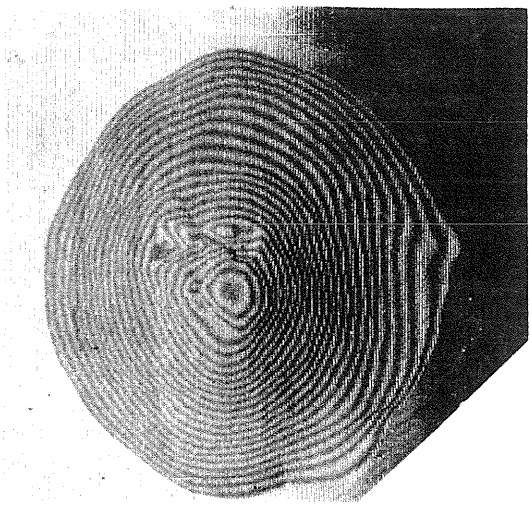

Figure 3. Moiré photograph of a conical pile used for angle of repose measurements. The contour lines are 1.4 mm apart in elevation.

equation (2) with C=0.013, which means the flow in the wind tunnel, though fully turbulent, is less turbulent than full scale.

Mass Flux Measurement

We installed a particle trap to measure mass transport (see Fig. 1). It consists of a recess in the floor well downstream of the test area. About 95 percent of the beads are trapped in this recess. We placed a filter-fabric bag downstream of the recess to capture all particles carried beyond the trap. The mass flux was determined by measuring the amount of mass collected over a given time, and normalized by tunnel width.

Drift Topography Measurement

Anno and Konshi (1981), and Wang (1989) have shown that moiré photography is an effective way to measure three-dimensional drift topography. This technique produces a photograph with topographic contour lines that represent the relief of the object. We use the shadow moiré technique described by Meadows et al.(1970). Basically, we project light through a fine grid onto the snow field and photograph through the same grid. Interference between the grid and its shadow yields a moiré image directly on the film plane. We digitize the resulting photographs using conventional digitizing systems. Figure 3 shows a moiré photograph taken in the SDWT.

SNOWDRIFT MODELING MEDIUM

The original activated clay used in the wind tunnel produced very realistic snowdrift patterns due to its high angle of repose, yet it has several drawbacks. The clay particles have threshold velocities well above their fall velocities; thus, as soon as the clay moves, it becomes fully entrained in the flow with turbulent diffusion dominating through all velocity regimes. Consequently requirements 4 and 5 cannot be satisfied simultaneously, and it is also impossible to study drift development because the clay completely obscures all activity in the wind tunnel. Furthermore, these particles easily escape the wind tunnel and become an inhalation hazard that we cannot satisfactorily mitigate.

We replaced the activated clay with glass beads similar to those used by Iversen (1979). The properties of these beads and those of naturally occurring wind-blown snow are listed in Table 1. As shown, the beads meet requirements 4 and 5 simultaneously because u_f/u_{*t} is about the same as for snow. Since Z'_{op}/Z'_{om}~2 to 290 requirement 2 can also be satisfied provided a scale factor in the range of 2 to 290 is selected. However, the threshold velocities are about the same for the beads and for snow. Thus, the Froude number will be distorted.

Figure 4 shows the average mass flux of the beads as a function of wind speed. The beads show a very predictable response with wind speed. This is unlike the full-scale situation, where mass flux may vary by several orders of magnitude for the sames wind speed, e.g., Kobayashi (1972), Takeuchi (1980), Schmidt (1986), Pomeroy (1988) and Tabler et al. (1990). Nevertheless, Figure 4 permits time scaling of drift development, provided field

Table 1. Comparison of bead properties to snow.

	Average Bead Size (μm)		
	57	*80*	*Dry Snow*
Density, σ (g/cc)	2.44	2.44	0.7
Mass Average Diameter, d (μm)	57	80	150*
Diameter Range (μm)	40 to 80	60 to 106	20 to 400**
Aerodynamic Roughness, Z_0 (cm)	$6.1x10^{-4}$ to $1.0x10^{-3}$	$3.8x10^{-3}$	10^{-3} -10^{-2}**
Saltation Roughness, Z_0' (cm)	$2.0x10^{-3}$ to $5.6x10^{-3}$	$3.4x10^{-3}$ to $6.9x10^{-3}$	$1.2x10^{-2}$ -$5.8x10^{-1}$§
Threshold Friction Velocity, $u*_t$ (m/s)	0.17	0.16	0.14* to 0.25¤
Average Terminal Velocity, u_f (m/s)	0.24	0.37	0.36*
$u_f/u*_t$	1.4	2.3	1.4 to 2.6
Angle of Repose, α (degrees.)	21 to 31	19 to 32	40 to 45§

*Iversen (1979), **Mellor (1965), §Kuroiwa (1967), ¤Pomeroy and Gray (1990)

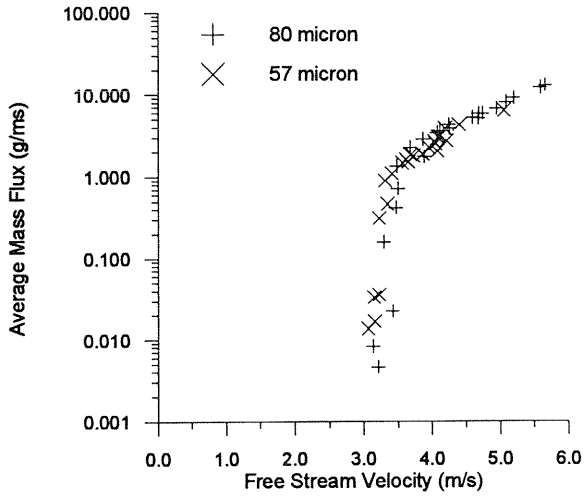

Figure 4. Mass transport of the glass beads.

values of mass flux are known, and any differences in capture efficiency between model and prototype are accounted for through calibration.

VERIFICATION TESTS

We conducted a series of preliminary verification tests using several simple structures and compared the resulting drifts with available field data. The structures included a Wyoming snow fence (1:150 scale), a leeward facing step (~1:60 to 1:100), several cylinders (1:4 to 1:10), and some rectangular prisms (1:50 to 1:80). All tests were run at U/U_t=1.15. The snow fence was run with a nonerodible bed (snow depth = 0) as the initial boundary condition. The step tests and three-dimensional bodies were run with both erodible (snow depth > 0) and nonerodible beds as the initial boundary conditions. The drift geometry was measured using moiré photography.

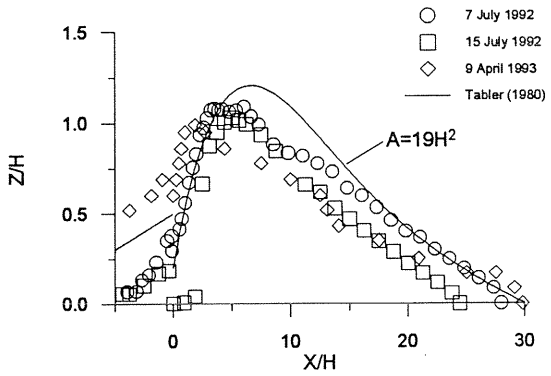

Figure 5. Equilibrium drift profile behind 1:150 model snow fence measured in the SDWT.

RESULTS AND DISCUSSION OF RESULTS

We first sought to confirm similitude between model and prototype equilibrium drift geometry for a snow fence. Figure 5 shows the equilibrium drift profile for the model snow fence compared with field data from Tabler (1980a). The vertical, Z, and horizontal, X, drift dimensions are normalized by fence height, H. The symbols represent data taken in the wind tunnel and the line is Tabler's fit to his field data. Although there is some discrepancy, our data fall well within the scatter seen in Tabler's field data.

We next sought to compare model and prototype snow fences for intermediate stages of drift development. Tabler (1980a) empirically determined that the leeward drift cross-sectional area at equilibrium is ~$19H^2$ and called this the fence capacity. This is the area enclosed by the solid line in figure 5. Taking the instantaneous cross-

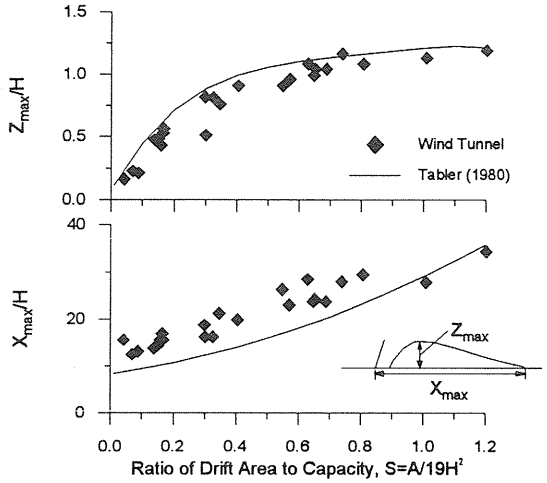

Figure 6. Results of snow fence tests in SDWT compared to those of Tabler (1980a).

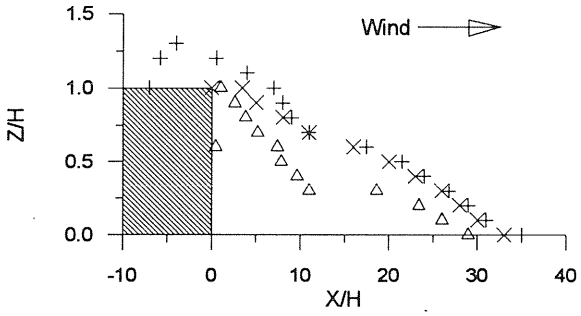

Figure 7. Leeward facing step test results.

sectional area, A, and normalizing it by the fence capacity gives a capacity fraction

$$S = \frac{A}{19H^2}. \qquad (7)$$

Tabler (1980a) plotted intermediate drift shapes for various values of S, and we did likewise. Figure 6 shows maximum drift length, X_{max}, and the drift height, Z_{max}, both normalized by fence height, plotted as a function of S. The average of Tabler's full-scale data is shown with the solid line, and the symbols are model data. Again our data agree reasonably well with those of Tabler. This does not confirm that the rate of filling of the model and prototype are similar, only that the intermediate geometries are similar.

A snow fence is a porous structure, and snow is transported around it differently than a solid structure. A solid two-dimensional structure for which some field data are available is a leeward facing step, so we tested this also. Figure 7 shows

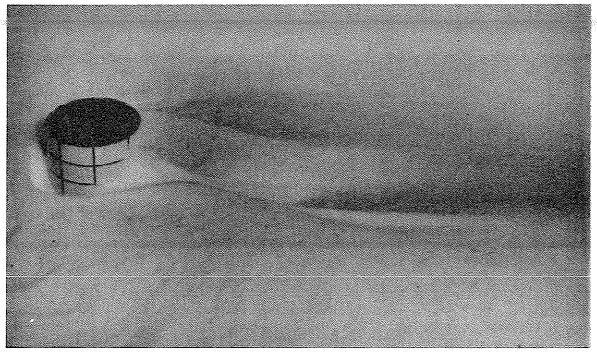

(a)

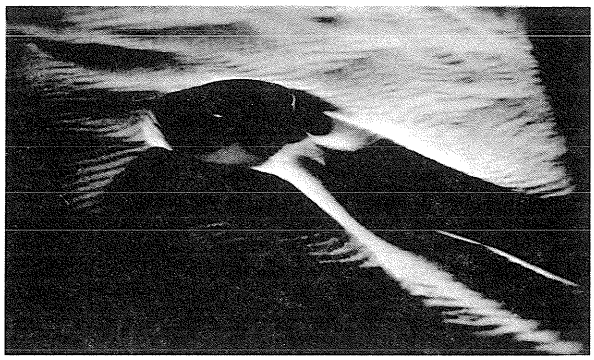

(b)

Figure 8. Snowdrift around right circular cylinder: (a) field, and (b) wind tunnel.

the equilibrium drift profile for the model tests of a leeward facing step. The vertical and horizontal drift dimensions are normalized by the step height, H. The drift length is about 30H, which is very similar to the results of a snow fence. Also, Tabler (1975) suggests that for drifts behind steps, the length at equilibrium is 20 to 40H for small steps (< 5 m) converging to 6.5H for tall steps (> 20 m). This height dependence reported by Tabler is an unexpected result, but perhaps the time it takes for large steps to reach equilibrium in the field is much longer than a winter season. Nevertheless, our results agree well with those of Tabler for small steps.

We also examined snow drifting around two simple three-dimensional objects: a right circular cylinder and a rectangular prism. To verify our results, we gathered field data on an ice-covered lake during the 1992-93 winter season.

Figure 8a shows a picture of a drift formed around a right circular cylinder in the field. Figure 8b shows a 1:4.4 scaled version in the wind tunnel. The general similarity of the windward trench and leeward ridge is evident between the model and prototype drifts.

To compare quantitatively the model and field

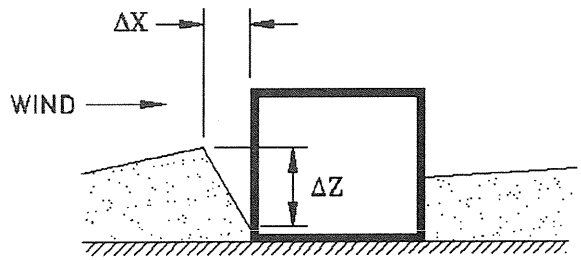

Figure 9. Schematic of drift geometry around three-dimensional objects.

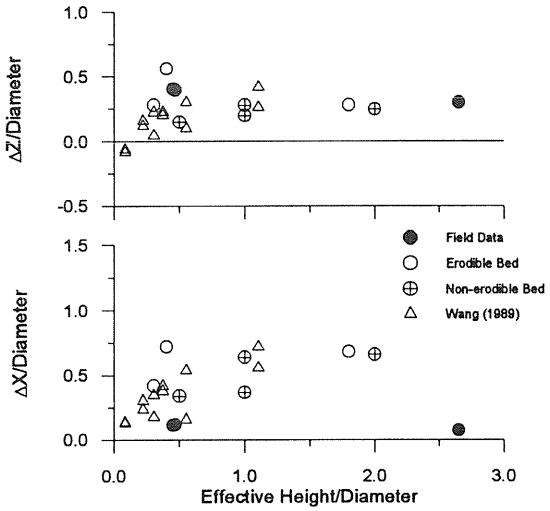

Figure 10. Right circular cylinder test results.

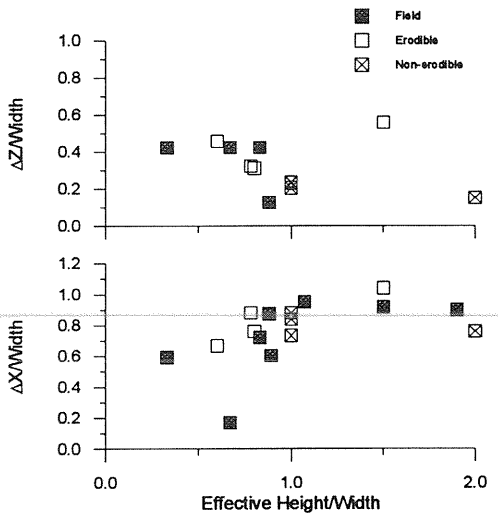

Figure 11. Rectangular prism test results.

data, we define two geometric parameters: the gap distance, ΔX, which is the distance from the front of the object to the windward cornice, and the mote depth, ΔZ, which is the depth of the windward scour hole. These parameters are shown in Figure 9. Although these are only two of many parameters that characterize a three-dimensional drift we used these because comparable lab data from Wang (1989) are available to supplement our sparse field data. We plotted these parameters against effective object height (the initial height the object protrudes above the snow) and normalized all dimensions by the diameter or width.

Figure 10 shows the results for the circular cylinders. Our data agree quite well with the model data of Wang (1989) who used sand as the modeling medium. There is also reasonable agreement between model and prototype for the mote depth, but the gap distance for the field data is substantially smaller than the model data. This discrepancy may be due to the smaller angle of repose of the beads compared with snow. However, we clearly require more field data to resolve this difference.

Figure 11 shows the results for the rectangular prisms. Here again we see a lot of scatter in the data for both model and prototype. However, for this case, the model and prototype show somewhat better agreement with respect to overall trends. Again, we require more field data to assess model results more thouroughly.

In the field we observed fundamentally different drift patterns around similar objects depending on whether the snow surface was erodible or nonerodible. We ran several model tests to study this effect. The drift geometry shown in Figure 8 was for an erodible bed in both the field and model cases. Figure 12 shows the corresponding surface plot of the model drift. Here erosion and deposition influence the final drift geometry. Figure 13 is surface plot for the nonerodible case. This feature is formed by deposition only. The differences between Figures 12 and 13 reflect what we have seen in the field and appear to be linked to the initial bed condition.

In principle this raises another similitude requirement: preservation of bed condition. However, deposition, not erosion, typically causes the majority of snow drifting problems and use of a nonerodible bed may be adiquate for most model studies. This approach may be justified based on the results in figures 10 and 11 where the windward features of mote depth and gap distance are virtually the same for both bed conditions. However, the

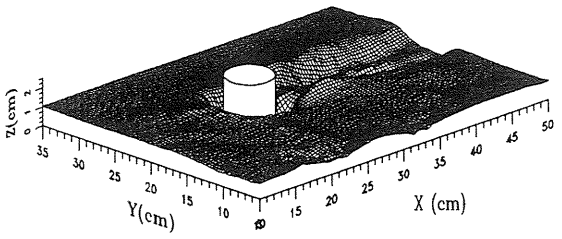

Figure 12. Surface plot of drift geometry around a right circular cylinder with an erodible bed.

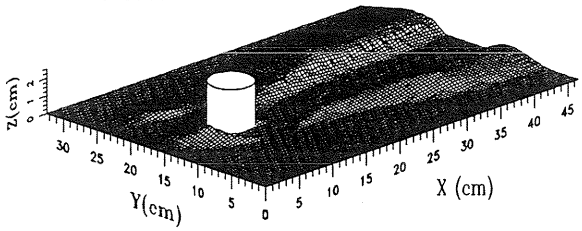

Figure 13. Surface plot of drift geometry around a right circular cylinder with a non-erodible bed.

leeward features are very different between Figures 12 and 13. We plan to study this issue further in both model and field tests.

CONCLUSIONS AND RECOMMENDATIONS

We modified the Snow Drifting Wind Tunnel at CRREL to achieve a flow field that replicates the planetary boundary layer. We also used glass beads as the model snow material. These changes allowed us to satisfy reasonably well five of the six principal scaling laws for snowdrift similitude. Only Froude number is significantly distorted. The minimum geometric scale for which the particles are expected to provide good similitude is 1:290. The scale factors used in this preliminary study ranged from 1:4 to 1:150.

A lack of field data for snow drifting around objects other than snow fences made detailed comparisons between model and prototype drifts difficult. Nevertheless, we found generally good agreement for both equilibrium and intermediate drift geometries around our model snow fence in comparison with well established field data. Furthermore, our model results for a two-dimensional step, a right circular cylinder, and a rectangular prism agree reasonably well with the scarce field results available and previous model tests using sand. We also explored the effects of erodible versus non-erodible initial conditions on drift formation. Preliminary field and model results show these effects to be significant.

Overall, we are satisfied with our modeling approach within the level of verification currently possible. Unfortunately, a general lack of quantitative field results limits verification of all snowdrift modeling, including the approach described here. Detailed full-scale snowdrift data essentially only exist for snow fences. However, their rates of development are not known.

To be effective, snowdrift modeling must correctly predict drift geometries and their rates of development. We require full-scale data to assess both of these requirements. As a minimum, we require equilibrium full-scale snowdrift geometries around simple two- and three-dimensional objects. To validate time scaling of model results, we require such measurements simultaneous with measurements of incident snow flux. These are ambitious needs, but without such data all modeling formulations cannot be completely validated.

ACKNOWLEDGMENTS

The authors gratefully acknowledge the help of Colleen Haehnel, Robert Demars, John Gagnon, Gary Koh, and Nancy Greeley, who gave support to this project.

REFERENCES

Anno, Y., "CRREL's Snowdrift Wind Tunnel," Cold Regions Technology Conf., 3rd, Sapporo Japan, Nov. 1987, pp. 405-410.

Anno, Y., "Requirements for Modeling of Snow Drift," *Cold Regions Science and Technology*, Vol. 8. (1984), pp. 241-252.

Anno, Y., and T. Konshi, "Modeling the Effects of a Snowdrift-preventing Forest and a Snow Fence by Means of Activated Clay Particles," *Cold Regions Science and Technology,* Vol. 5 (1981), pp. 43-58.

Iversen, J. D., "Drifting Snow Similitude," *Journal of Hydraulics Division,* ASCE, Vol. 105, No. HY6, Proc. Paper 14647, June 1979, pp. 737-753.

Kind, R. J., "A Critical Examination of the Requirements for Model Simulation of Wind-induced Erosion/Deposition Phenomenon such as Snow Drifting," *Atmospheric Environment,* Pergamon Press, Vol. 10, (1976), pp. 219-227.

Kind, R. J., "Snow Drifting, " *Handbook of Snow , Principles, Processes, Management, and Use,* eds. D. M. Gray and D. H. Male, Pergamon Press, Toronto (1981).

Kind, R. J., "Snow Drifting: A Review of Modeling Methods," *Cold Regions Science and Technology*, Vol. 12, (1986), pp. 217-228.

Kobayashi, D., "Studies of Snow Transport in Low-level Drifting Snow," Institute of Low Temperature Science, July 1972.

Kuroiwa, D. ,Y. Mizuno, and M. Takeuchi, "Micromeritical Properties of Snow", *Physics of Snow and Ice,* International Conference on Low Temperature Science, Sapporo, Japan, (1967).

Meadows, D. M. , W. O. Johnson, and J. B. Allen , "Generation of Surface Contours by Moiré Patterns," *Applied Optics,* Vol. 9, No. 4, April 1970, pp. 942-7.

Mellor, M., *Blowing Snow,* Report III-A3c, Cold Regions Science and Engineering Monograph, U.S. Army Cold Regions Research and Engineering Laboratory, Hanover, NH, 1965.

Pomeroy, J. W., "Wind Transport of Snow," Ph.D. Thesis, Division of Hydrology, University of Saskatchewan, Saskatoon, (1988).

Pomeroy, J. W., and D. M. Gray, "Saltation of Snow," *Water Resources Research*, Vol. 26, No 7, July 1990, pp. 1583-1594.

Schmidt, R. A., "Threshold Wind-Speeds and Elastic Impact in Snow Transport," *Journal of Glaciology,* Vol. 26, No. 94, (1980), pp. 453-467.

Schmidt, R. A., "Transport Rate of Drifting Snow and the Mean Wind Speed Profile," *Boundary Layer Meteorology,* Vol. 34, (1986).

Simiu, E., and R. H. Scanlan, *Wind Effects on Structures: An Introduction to Wind Engineering,* John Wiley and Sons, New York (1978).

Tabler, R. D., "Predicting Profiles of Snowdrifts in Topographic Catchments," *Proc. Western Snow Conf.*, Coronado, CA, (1975).

Tabler, R. D., "Geometry and Density of Snow Drifts Formed by Snow Fences," *Journal of Glaciology,* Vol. 26, No. 94, (1980a).

Tabler, R. D., "Self-Similarity of Wind Profiles in Blowing Snow Allows Outdoor Modeling," *Journal of Glaciology*, Vol. 26, No. 94, (1980b)

Tabler, R. D., J. W. Pomeroy, and B. W. Santana, "Drifting Snow," *Cold Regions Hydrology and Hydraulics,* ASCE, (1990).

Takeuchi, M., "Vertical Profile and Horizontal Increase of Drift-Snow Transport," *Journal of Glaciology,* Vol. 26, No. 94 (1980).

Teunissen, H. W., *Characteristics of Mean Wind and Turbulence in the Planetary Boundary Layer,* University of Toronto, UTIAS Review No. 32, October, 1970.

Wang, W., Saltation topographic phenomenon: The Moiré fringe technique, Masters Thesis, University of Iowa, Ames, Iowa (1989).

Wuebben, J. L., "A Hydraulic Model Investigation of Drifting Snow," CRREL Report 78-16, Cold regions Research and Engineering Laboratory, Hanover, NH (1978).